IEICE TRANSACTIONS

on Fundamentals of Electronics, Communications and Computer Sciences

VOL. E102-A NO. 1
JANUARY 2019

A PUBLICATION OF THE ENGINEERING SCIENCES SOCIETY
The Institute of Electronics, Information and Communication Engineers
Kikai-Shinko-Kaikan Bldg., 5-8, Shibakoen 3 chome, Minato-ku, TOKYO, 105-0011 JAPAN

PAPER

Phase-Difference Compensation and Nonuniform Pulse Transmission for Accurate Real-Time Moving Object Tracking

Koichi ICHIGE[†a)], ***Member***, **Nobuya ARAKAWA**[††], ***Nonmember***, **Ryo SAITO**[†], ***Student Member***, ***and*** **Osamu SHIBATA**[††], ***Member***

SUMMARY This paper presents a radio-based real-time moving object tracking method based on Kalman filtering using a phase-difference compensation technique and a non-uniform pulse transmission scheme. Conventional Kalman-based tracking methods often require time, amplitude, phase information and their derivatives for each receiver antenna; however, their location estimation accuracy does not become good even with many transmitting pulses. The presented method employs relative phase-difference information and a non-uniform pulse generation scheme, which can greatly reduce the number of transmitting pulses while preserving the tracking accuracy. Its performance is evaluated in comparison with that of conventional methods.

key words: *location estimation, tracking, Kalman filter*

1. Introduction

Moving object tracking [1], [2] is a significant technique in wireless communication applications like mobile terminal position detection, and now is also used for many different kinds of applications. One of these is in the field of sports, where the players can be regarded as moving objects. Important incidents occurring during a game often cannot be recognized either by the human eye or by using state-of-the-art camera techniques. Therefore, accurate tracking of moving players has become important for football game analysis.

There exist some video-based moving object tracking systems [3]–[6] that are already used for training and game analysis. However, due to problems with low or blocked visibility, these systems need manual intervention and a long processing time to deliver data on a limited level of detail. Hence a radio-based tracking system [7] has also been studied for accurate tracking of moving players. This approach is basically based on Kalman filtering [8], with delay time, amplitude, carrier phase information and their derivatives for each antenna element, and detects the target location using TOA (time of arrival) and TDOA (time difference of arrival) information. However, the system consumes a large amount of power because it transmits hundreds or thousands of pulses per second.

Manuscript received February 21, 2018.
Manuscript revised July 12, 2018.

[†]The authors are with Department of Electrical and Computer Engineering, Yokohama National University, Yokohama-shi, 240-8501 Japan.
[††]The authors are with Murata Manufacturing Co., Ltd., Nagaokakyo-shi, 617-8555 Japan.
a) E-mail: koichi@ynu.ac.jp

DOI: 10.1587/transfun.E102.A.211

Besides, methods for tracking moving objects using TDOA-based Kalman filtering have been reported in the literature [9], [10]. The approach cited in [9] can track moving objects but its main target is to detect either LOS (line-of-sight) or NLOS (non-LOS) environments. The approach cited in [10] requires a large number of antenna elements and installs them in a very wide area. Kalman-based tracking approaches for wireless sensor networks have also been reported [11], [12]. However they have some drawbacks like low tracking accuracy or large computational cost.

In this paper, we present a novel, accurate, low-cost, radio-based moving object tracking method based on Kalman filtering, which uses a phase-difference compensation technique and a non-uniform pulse transmission scheme [13]. With the method, better location detection accuracy is obtained by using the phase-difference information between antenna elements as one of the state vector elements in Kalman filtering. We employed a non-uniform pulse configuration, which is generated and transmitted from moving objects, in order to correctly compensate for the phase difference even with a small number of transmitted pulses. We further developed the system by averaging TDOA values. We also evaluated the method's performance in comparison with that of conventional methods.

The rest of this paper is organized as follows. Section 2 briefly introduces the conventional Kalman-based approach [7]. Section 3 describes the proposed tracking method, first by detailing the state vector formulation in Kalman filtering and then by detailing the non-uniform pulse generation scheme for phase compensation. After showing some simulation results in Sect. 4, we make some concluding remarks in Sect. 5.

2. Preliminaries

In this section, we briefly review the conventional target tracking system [7] based on Kalman filtering.

2.1 System Model

The system consists of a set of small and lightweight transmitters (objects to be located) and a receiving infrastructure that is set up around the area of interest, which may be the inner part of a football stadium. The system's air interface employs the carrier frequency f_0 with a bandwidth around Δf. The system's miniature transmitters make use

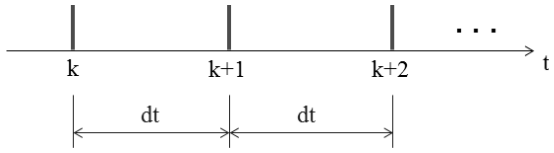

Fig. 1 Conventional pulse generation scheme.

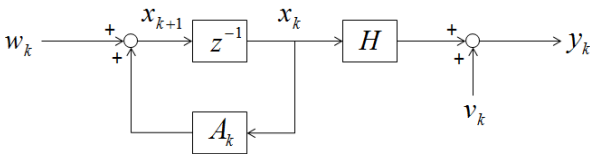

Fig. 2 Basic system model of Kalman filter.

of this bandwidth by generating short but broadband signal bursts of pulse-shaped sequences with the time interval dt as in Fig. 1. It is mentioned in [7] that the number of pulses $N = 1/dt$ per second should be larger than 200 for accurate 2-D tracking, however, more battery power will be spent for larger values of N. Therefore, smaller values of N are desired.

2.2 Kalman Filtering

This subsection briefly reviews the classical Kalman Filtering and its equations used in moving object tracking.

Kalman filter is an algorithm that first observes time series measurements containing statistical noise, and then estimates unknown variables by using Bayesian estimation over the variables for each timeframe [8]. Its basic system model can be illustrated as in Fig. 2, which can be formulated by

$$\begin{aligned} \boldsymbol{x}_{k+1} &= \boldsymbol{A}\boldsymbol{x}_k + \boldsymbol{v}_k, \\ \boldsymbol{y}_k &= \boldsymbol{H}\boldsymbol{x}_k + \boldsymbol{w}_k, \end{aligned}$$

where $\boldsymbol{x}_k$ and $\boldsymbol{y}_k$ respectively denote state and observation vectors, $\boldsymbol{A}$ and $\boldsymbol{H}$ denote state transition and observation matrices assumed to be known in advance, $\boldsymbol{v}_k$ and $\boldsymbol{w}_k$ denote process and observation noises both assumed to be zero mean and independent to each other. In Kalman filter theory, the process noise is determined depending on how much the priori estimates are reliable against the observation noise [8]. However, in real situation, the value of the process noise is empirically determined so that the Kalman filter works effectively.

The estimation process of the Kalman filter can be divided into two parts: "predict" and "update" [8]. The prediction part uses the state estimate from the previous timestep to produce an estimate of the state at the current timestep. Then in the update part, the current (priori) prediction is combined with current observation information to refine the state estimate. That improved estimate is termed the updated (posteriori) state estimate.

In the prediction part, the priori estimation procedure at the time $t = kdt$ can be formulated as

$$\begin{aligned} \bar{\boldsymbol{x}}_k &= \boldsymbol{A}\hat{\boldsymbol{x}}_{k-1}, \\ \bar{\boldsymbol{P}}_k &= \boldsymbol{A}\boldsymbol{P}_{k-1}\boldsymbol{A} + \boldsymbol{Q}, \end{aligned} \tag{1}$$

where $\bar{\boldsymbol{x}}_k$ and $\hat{\boldsymbol{x}}_k$ respectively denote the priori and posteriori estimates of the state vector $\boldsymbol{x}_k$. Besides, the matrices $\boldsymbol{P}$ and $\boldsymbol{Q}$ denote the posteriori and process error covariances.

In the update part, the posteriori estimation procedure can be formulated as

$$\begin{aligned} \boldsymbol{K}_k &= \bar{\boldsymbol{P}}_k\boldsymbol{H}^T(\boldsymbol{H}\bar{\boldsymbol{P}}_k\boldsymbol{H}^T + \boldsymbol{R})^{-1}, \\ \hat{\boldsymbol{x}}_k &= \bar{\boldsymbol{x}}_k + \boldsymbol{K}_k(\boldsymbol{z}_k - \boldsymbol{H}\bar{\boldsymbol{x}}_k), \\ \boldsymbol{P}_k &= (\boldsymbol{I} - \boldsymbol{K}_k\boldsymbol{H})\bar{\boldsymbol{P}}_k, \end{aligned}$$

where the matrix $\boldsymbol{R}$ denotes the observation noise covariance, and the value $\boldsymbol{K}_k$ is the Kalman gain. Then return to (1) and update the parameters at the time of $t = (k+1)dt$.

2.3 Conventional Approach

Suppose that we have L receiver antennas used for moving object tracking. The conventional system cited in [7] tracks the moving objects based on Kalman filtering [8], with its state vector at the time $t = kdt$:

$$\boldsymbol{x}_k = \left[\boldsymbol{x}_{1,k}^T, \boldsymbol{x}_{2,k}^T, \ldots, \boldsymbol{x}_{L,k}^T\right]^T, \tag{2}$$

$$\boldsymbol{x}_{i,k} = \left[t_{i,k}, M_{i,k}, \phi_{i,k}, \dot{t}_{i,k}, \dot{\phi}_{i,k}\right]^T, \quad i = 1, 2, \ldots, L, \tag{3}$$

where $t_{i,k}, M_{i,k}, \phi_{i,k}$ respectively denote the delay time (TDOAs), amplitude, and carrier phase, with two derivatives for delay time $\dot{t}_i$ and for carrier phase $\dot{\phi}_{i,k}$ at the i-th receiver antenna element. The magnitude and phase terms in (3) are used to suppress multipath components as mentioned in [7]. If they are negligible, the vector (3) can be reduced to

$$\boldsymbol{x}_{i,k} = \begin{bmatrix} t_{i,k} \\ \dot{t}_{i,k} \end{bmatrix}, \quad i = 1, 2, \ldots, L, \tag{4}$$

with the state and observation matrices $\boldsymbol{A}$ and $\boldsymbol{H}$:

$$\boldsymbol{A} = \begin{bmatrix} 1 & dt \\ 0 & 1 \end{bmatrix},$$

$$\boldsymbol{H} = \begin{bmatrix} 1 & 0 \end{bmatrix}.$$

Since the delay time $t_{i,k}$ and its derivative $\dot{t}_{i,k}$ terms in (4) are affected by the same noise, the priori estimate in Kalman filtering cannot be accurate. Moreover, the state vector $\boldsymbol{x}_k$ in (2) contains the information of all the L receiving antennas, which requires large computational cost in Kalman filtering.

Once TDOAs are estimated by Kalman filtering, the player position can be specified as an intersection of hyperbolas [1], [7] as illustrated in Fig. 3. It can be uniquely specified in the case of 2 anchors but cannot be specified in the case of more than 2 anchors. Least square method is employed to specify it from its multiple candidates.

3. Proposed Approach

In this section, we describe the proposed tracking method,

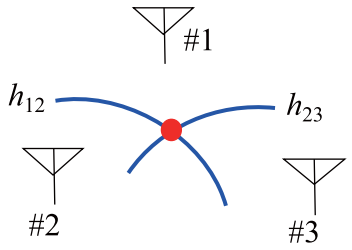

Fig. 3 Detection of player position as an intersection of hyperbolas.

first by detailing the state vector formulation in Kalman filtering, and then by detailing the non-uniform pulse generation scheme for phase-difference compensation.

3.1 State Vector with Phase Difference

We newly introduce the phase-difference information into the state vector in Kalman filtering, instead of the absolute phase characteristics of each antenna used in (3). Here we employ the relative phase difference between antenna elements, and also replace the delay time index with the TDOA between antenna elements.

Let $t_{mn,k}$ $(m, n = 1, 2, \ldots, L,\ m < n)$ denote the TDOA between the antennas #m and #n. From the TDOAs, for example from $t_{12,k}$ and $t_{23,k}$, we can estimate the target location as an intersection of two hyperbolic tracking functions. First the state vector in (4) is modified by using TDOA values, i.e.

$$\boldsymbol{x}_{mn,k} = \begin{bmatrix} t_{mn,k} \\ \dot{t}_{mn,k} \end{bmatrix}, \tag{5}$$

with the state transition matrix:

$$\boldsymbol{A} = \begin{bmatrix} 1 & dt \\ 0 & 1 \end{bmatrix},$$

We do not combine the state information of receiver antennas; the TDOA values between two antennas are individually updated by Kalman filtering.

Then we replace the derivative $\dot{t}_{mn,k}$ with the relative phase difference information. The state vector in (5) can be further modified into

$$\boldsymbol{x}_{mn,k} = \begin{bmatrix} t_{mn,k} \\ \Delta\phi_{mn,k} \end{bmatrix}, \tag{6}$$

where $\Delta\phi_{mn,k}$ is the relative phase difference between the m-th and n-th antenna elements during the time from $(k-1)dt$ to kdt. The state vector (6) can be further modified to include the derivative of the phase difference $\Delta\dot{\phi}_{mn,k}$:

$$\boldsymbol{x}_{mn,k} = \begin{bmatrix} t_{mn,k} \\ \Delta\phi_{mn,k} \\ \Delta\dot{\phi}_{mn,k} \end{bmatrix}. \tag{7}$$

In this case, the state transition matrix $\boldsymbol{A}$ and the observation matrix $\boldsymbol{H}$ in the Kalman filter can be written as follows.

$$\boldsymbol{A} = \begin{bmatrix} 1 & \dfrac{1}{\omega_0} & \dfrac{dt}{2\omega_0} \\ 0 & 1 & dt \\ 0 & 0 & 1 \end{bmatrix},$$

$$\boldsymbol{H} = \begin{bmatrix} 1 & 0 & 0 \\ 0 & 1 & 0 \end{bmatrix}.$$

where $\omega_0 = 2\pi f_0$ is the angular carrier frequency. Note that the location estimation error will be reduced by using the phase-difference information, since the error in time is divided into amplitude and phase terms, and therefore the phase-difference information would be affected only by phase error but would not be affected by amplitude error. From our simulation results described in the next section, we found that error components mainly remain in the amplitude characteristics and do not seriously affect the phase-difference characteristics. Therefore, we employ these characteristics in addition to the TDOA information.

The anchors are paired into every three combinations because at least three anchors are required to estimate player's location [1], [7]. In case of 4 anchors (#1, #2, #3, #4), the number of pairs would become ${}_4C_3 = 4$, and the possible combinations are (#1, #2, #3), (#1, #2, #4), (#1, #3, #4) and (#2, #3, #4). In a similar manner, the number of pairs will become ${}_MC_3$ in case of M anchors.

3.2 Non-Uniform Pulse Generation

There is still a problem with the proposed state vector (7), i.e. we cannot specify phase differences that are out of the range $[-\pi, \pi]$. For example, once we have observed the phase difference $\phi = \pi/2$, we have no idea if the true phase information is $\phi = \pi/2$, $\phi = \pi/2 \pm 2n\pi, or\ n = \pm1, \pm2, \ldots$. This happens when we use large carrier frequency f_0 or a small number of samples N per second. Indeed, the smaller number of samples N is important for achieving lower transmitter power consumption. As the power consumption is proportional to the number of transmitted pulses, reducing the number of pulse transmission will directly affect to power consumption.

To correctly estimate the phase difference out of $[-\pi, \pi]$, we employ a non-uniform pulse configuration that is generated and transmitted from the miniature moving objects as illustrated in Fig. 4 instead of the uniform pulse configuration in Fig. 1, where dp denotes the fine pulse interval [13]. The additional pulses at the time $t = kdt + dp, (k+1)dt+dp, \ldots$ in Fig. 4 are used to correctly estimate the phase difference out of $[-\pi, \pi]$. Figure 5 illustrates the way of estimating next phase-difference information in the proposed method, using nonuniform pulses. The conventional method [7] should satisfy that the phase difference at dt should be within $\pm\pi$, therefore the value of dt must be very small. On the other hand, the proposed method requires the condition that the phase difference at dp should be within $\pm\pi$, and then the phase at the time dt can be estimated by linear prediction. In this manner, the proposed method can correspond to

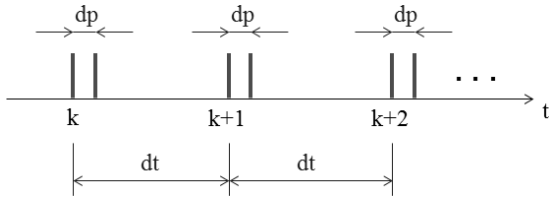

Fig. 4 Proposed pulse generation scheme.

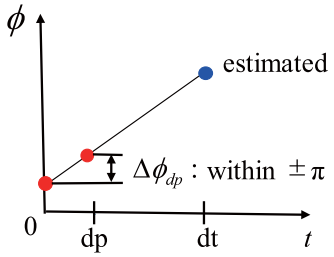

Fig. 5 Estimation of next phase-difference information using nonuniform pulses.

larger values of dt.

The way of compensating phase difference for the additional pulses is summarized as follows. Let $\lambda = f_0/c$ denote the wavelength of the carrier signal, where c denotes the velocity of light. Assume a moving target with the maximum velocity $v_{\max}$, then the distance moved within the fine pulse interval dp becomes $v_{\max} \cdot dp$ [13]. Then the carrier phase difference will become within $[-\pi, \pi]$ provided that the distance $v_{\max} \cdot dp$ becomes less than the half-wavelength $\lambda/2$. Therefore the fine pulse interval dp is determined so as to satisfy

$$dp < \frac{\lambda}{2v_{\max}}. \tag{8}$$

We again use the same state vector (7) for Kalman filtering, but now $\Delta\phi_{mn,k}$ denotes the relative phase difference between the m-th and n-th antenna elements during the time from kdt to $kdt + dp$, not from $(k-1)dt$ to kdt. Therefore the state vector (7) can be used but the state transition matrix $\boldsymbol{A}$ is modified as

$$\boldsymbol{A} = \begin{bmatrix} 1 & \frac{1}{\omega_0} \cdot \frac{dt}{dp} & \frac{1}{2\omega_0} \cdot \frac{dt^2}{dp} \\ 0 & 1 & dt \\ 0 & 0 & 1 \end{bmatrix}.$$

Note that the computational cost may become larger than the conventional method because of a 3-element state vector, while the conventional method uses a 2-element state vector. The increment of the computational load would be around 60% due to the larger size of matrices and vectors. However, the size of matrices and vectors are basically all small, maximum 3×3 matrix operations as described in Sect. 2.2. Those operations could be executed within a very short time; there is no any iterative operation or optimization process. Therefore we can easily update the state vectors within a pulse duration dt.

3.3 Tuning TDOA Values by Averaging

The location estimation accuracy is further enhanced by averaging TDOA values. Using the non-uniform pulses in Fig. 4, we can observe multiple TDOA values $t_{mn,k}$ and $t_{mn,k+dp}$ as well as the phase difference. Then we calculate the average of the TDOA values:

$$\hat{t}_{mn,k+\frac{dp}{2}} = \frac{t_{mn,k} + t_{mn,k+dp}}{2}. \tag{9}$$

To suppress the noise effect, we hereafter use the above averaged TDOA $\hat{t}_{mn,k+\frac{dp}{2}}$ instead of $t_{mn,k}$.

Furthermore, the number of pulses within the interval dt is fixed to 2 as in Fig. 4 but it could be more than 2. Let P denote the number of pulses within the interval dt. Then the averaged TDOA can be written as

$$\begin{aligned} \hat{t}_{mn,k+\frac{(P-1)dp}{2}} &= \frac{t_{mn,k} + t_{mn,k+dp} + \cdots + t_{mn,k+(P-1)dp}}{P} \\ &= \frac{1}{P} \sum_{\ell=0}^{P-1} t_{mn,k+\ell dp}. \end{aligned} \tag{10}$$

The larger P will achieve better tracking accuracy due to noise suppression effect, which is confirmed in the next section.

4. Simulation

We used simulations to compare our proposed tracking method to the conventional method cited in [7].

4.1 Specifications

The specifications used in the simulations basically followed those cited in [7], but some were modified to clearly evaluate our method's effectiveness. The obtained results are summarized in Table 1. We assumed a football field of 100 m × 70 m as in Fig. 6, where the center, top-right, and bottom-left of the field were respectively specified as $(x, y) = (0, 0)$, $(50, 35)$ and $(-50, -35)$. Four receiver antennas were installed at $(60, 45)$, $(-60, 45)$, $(60, -45)$ and $(-60, -45)$, which were 10 m × 10 m removed from each edge of the field as in the figure. The air interface employed the ISM (industrial scientific medical) band at 2.4 GHz, allowing the usage of about 80 MHz. We assume the maximum velocity $v_{max} = 10$ m/sec, and it satisfies the condition (8) for the given specifications $\lambda = c/f_0 = 0.125$m, and $dp = 0.003$sec.

We evaluated the tracking accuracy of only one moving object, even though the method cited in [7] can track two or more objects. We found that multiple objects could be tracked more accurately when we distinguished multiple objects by code (e.g. Gold code). Here we assume that the shape of transmission signal from a tag is basically a pulse, or it could be a sequence with a particular length instead of

Table 1 Simulation specifications.

scenario	#1	#2
tested field	100 m×70 m (as in Fig. 6)	
no. of antennas L	4 (as in Fig. 6)	
no. of tags	1	
carrier frequency f_0	2.4 GHz	
occupied bandwidth Δf	80 MHz	
sampling frequency f_s	400 MHz	
SNR	23 dB	
CNR	20 dB	
maximum velocity $v_{\max}$	10 m/sec	
time detection error	Gaussian distribution with σ_t=0.723 nsec	
phase detection error	Gaussian distribution with σ_ϕ=4.05 deg	
coarse time interval dt	0.04 sec	
fine time interval dp	0.003 sec	
no. of iterations	251 (10 sec)	201 (8 sec)
model of moving objects	Fig. 7(a)	Fig. 7(b)
starting point of objects	(−2.5, −6)	(10, −5)

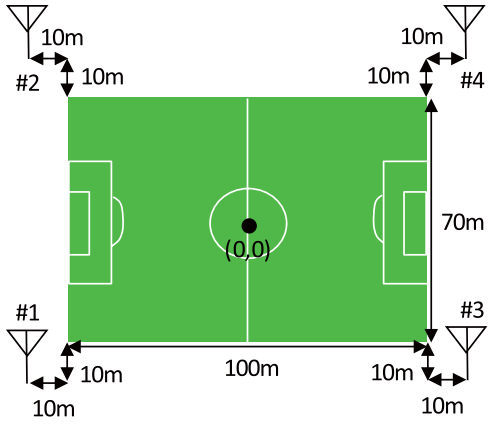

Fig. 6 Modeling of football field and measurement antennas.

the pulse shape. In that case, we can develop a system corresponding to multiple target case by employing individual sequences like M-sequence or Gold code as the transmission signal of individual tags, because the correlation of different sequences in those codes becomes small. Then at the later (receiver) stage, we can receive signal and then divide it into each tag component by correlating with ideal codes.

Assumed number of transmitters and receivers are as follows; we aim at analyzing football game, means that several tens of transmitters, i.e., 11 players×2 team + 3judges + 1 ball = 26 transmitters. Adding some others, we assume around 30 targets to be localized. The receivers could be 3 as a minimum, but it is not accurate because a triangle made by 3 antenna at any corner of football field cannot cover the whole field but can cover at most a half of it. Therefore 4 receivers would be minimum, otherwise 6 would be desired.

4.2 Target Model

We assumed the maximum moving velocity of football players was 10 m/sec, and tried to reduce the number of pulses N to 25 times a second so as to save transmitting power. If we had used the uniform pulse configuration as shown in Fig. 1, we would not have been able to track moving objects because the inequality (8) would not hold in that case. Therefore we employed the non-uniform pulse configuration shown in Fig. 4 with the fine pulse interval dp = 0.003 sec. Then the inequality (8) holds and therefore we could use Kalman filtering for accurate object tracking.

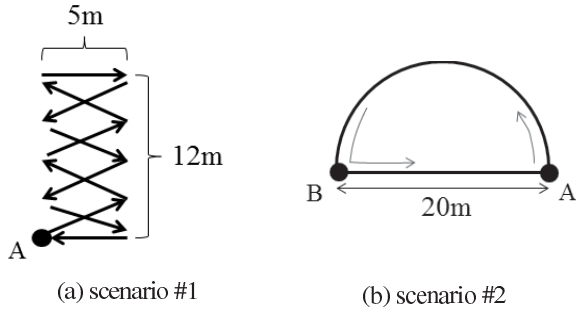

Fig. 7 Modelling of moving targets.

The tested motion models are illustrated in Fig. 7. In scenario #1, the object starts from 'A' and takes one second to follow each diagonal or horizontal line. Hence the total moving time is 10 seconds. In scenario #2, the object takes 4 seconds to follow the half-circle from 'A' to 'B', and then takes another 4 seconds to move straight from 'B' to 'A'. The time interval of Kalman filtering is set to 0.04 seconds (25 times per second). The reason of testing those two scenarios is to see if there is any difference between the motions along straight lines in Fig. 7(a) and curves in Fig. 7(b). Also it is more difficult to track moving objects than to estimate the location of static objects; i.e., how to determine the value of process noise, pulse interval, and so on.

Note that the method cited in [7] requires more than 1,000 Kalman filtering iterations per second for accurate tracking in the case of the specifications in Table 1. The proposed method requires 25 iterations per second, even the cost per iteration becomes 60% richer than the method [7]. Then the total computational cost of the proposed method per second will become only around 4.0% in comparison with the cost of [7] per second, which realizes much less computational cost than [7]. Note that the power consumption can be reduced as well.

In this case, the maximum moving distance per iteration is 40 cm; hence the carrier wavelength should be more than 80 cm. In other words, the carrier frequency should originally be set to 375 MHz or less. However, since we can compensate for the phase difference by using the method described in Sect. 3.2, the carrier frequency can be set to be 375 MHz or more. For these simulations it was set to 2.4 GHz.

4.3 Tracking Performance

Figures 8(a) and 8(b) respectively show the behavior of time

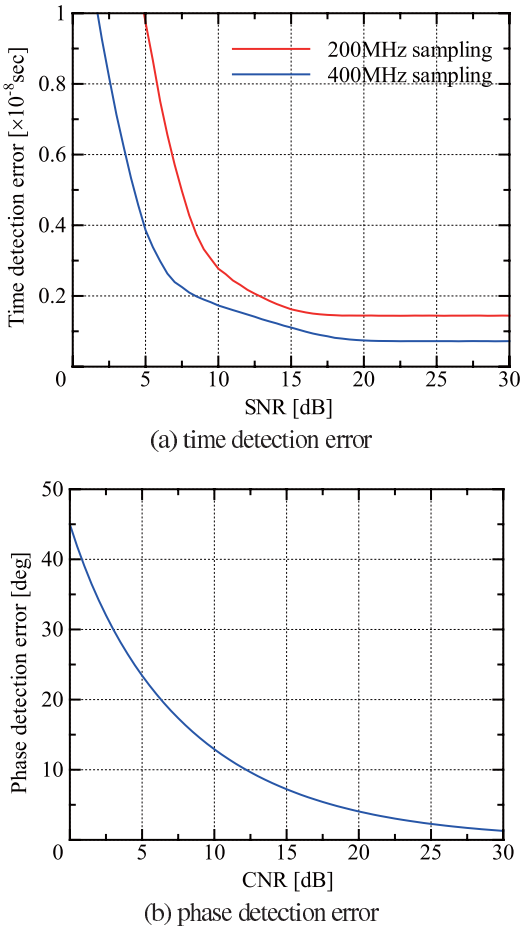

Fig. 8 Time and phase detection errors.

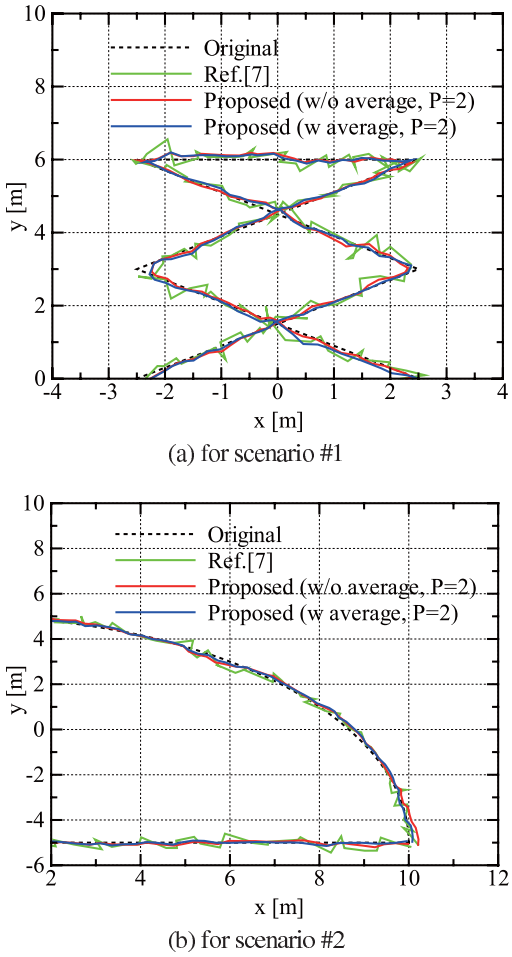

Fig. 9 Comparison of location tracking results for scenarios #1 and #2.

detection error as a function of SNR and that of phase detection error as a function of CNR, where the values of the process noise in Kalman filtering are $\sigma = 15$ in the proposed method and $\sigma = 5 \times 10^{-9}$ in the conventional method [7]. We see from Fig. 8 that larger SNR and CNR lead to smaller time and phase detection errors, which will improve the tracking accuracy. For a system with a sampling frequency of 400 MHz, 23 dB SNR, and 20 dB CNR, the time and phase detection errors will respectively become the normal Gaussian distribution with the standard deviation $\sigma_t = 0.723$ nsec and that with $\sigma_\phi = 4.05$ deg.

Figures 9(a) and 9(b) show the object tracking results. From them we can see that the proposed method well follows the original motion model, while the locations estimated using the conventional method often have large errors.

4.4 Tracking Error Analysis

Figures 10(a) and 10(b) show the moving object tracking accuracy results obtained by means of RMSE (root mean square error) as a function of time. From them we see from that the proposed method achieves the smallest RMSE overall while the conventional methods have large estimation errors. We confirmed from Fig. 10 that the proposed nonuniform pulse transmission and phase-difference compensation approaches work effectively.

We also compared the average RMSE obtained for scenarios #1 and #2 with the proposed method with those obtained with the methods cited in [7]. The results are summarized in Table 2. Table 2 shows that the proposed method achieved much better tracking accuracy than the method cited in [7], also better than the method [7] with 50 Hz, and also better results could be achieved with averaging and larger values of P.

Table 2 also indicates that a larger value of P leads to smaller error for both scenarios #1 and #2. To show the effect of P in more detail, we compare the average RMSE as a function of P for these scenarios in Fig. 11. It can be seen from Fig. 11 that the RMSE becomes smaller when P gets larger. This means that a larger P value achieves smaller tracking error but also requires larger power consumption. Since the RMSE behavior becomes inversely proportional to $\sqrt{P}$ as shown in Fig. 11, small values like $P = 2$ or 3 will consequently be adequate.

Also Fig. 12 shows the behaviors of time detection and position estimation errors by the proposed method versus

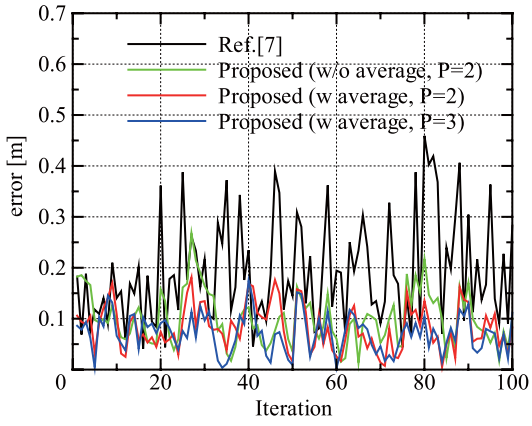

(a) for scenario #1

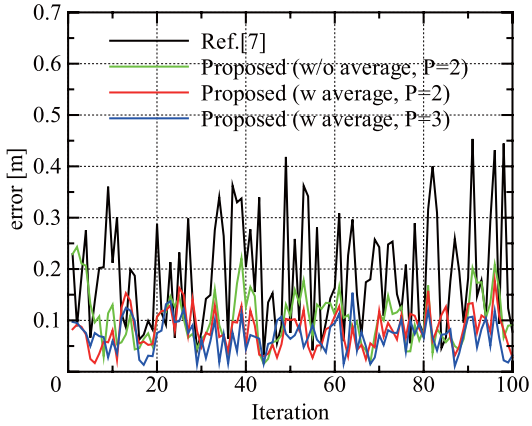

(b) for scenario #2

Fig. 10 Comparison of tracking errors for scenarios #1 and #2.

Table 2 Comparison of averaged RMSEs.

sce-nario	Ref. [7]		Proposed (25 Hz)		
	25 Hz	50 Hz	w/o average	w average	
			$P = 2$		$P = 3$
#1	0.226 m (100%)	0.148 m (65.4%)	0.103 m (45.5%)	0.0826 m (36.5%)	0.0724 m (31.9%)
#2	0.228 m (100%)	0.131 m (57.2%)	0.0945 m (41.5%)	0.0732 m (32.2%)	0.0647 m (28.4%)

SNR, when we do not use code division and track multiple tag locations together. We see from Fig. 12 that the error in multiple tags case is almost the same with that in a single tag case, even with 30 tags. From this fact, we can say that the multiple tag processing does not seriously affect to the tracking accuracy, almost comparable with a single tag case.

5. Concluding Remarks

In this paper, we described our development of a radio-based moving object tracking system using non-uniform pulse transmission and phase difference compensation. We showed how we averaged the observed neighboring TDOA values and in so doing were able to improve the tracking accuracy over that of a conventional method. Further improving tracking accuracy remains as a subject for future studies.

For hardware implementation, we can employ software defined radio (SDR) system like RF transceiver chips and wireless communication module using FPGA or microcomputer, which covers the ISM band at 2.4 GHz. The anchors

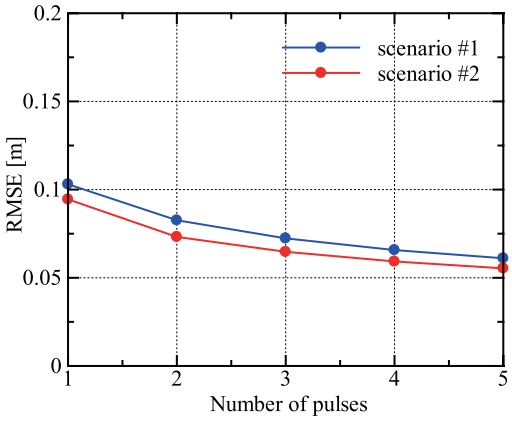

Fig. 11 Comparison of averaged RMSE as a function of P for scenarios #1 and #2.

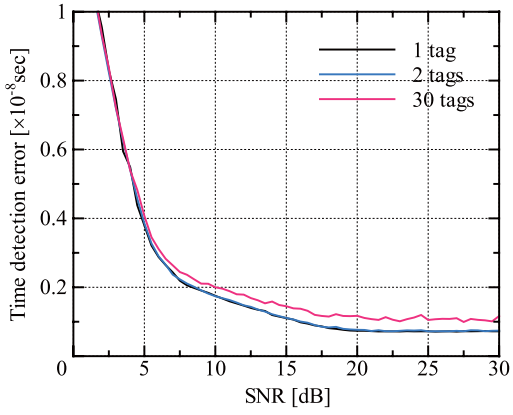

(a) time detection error

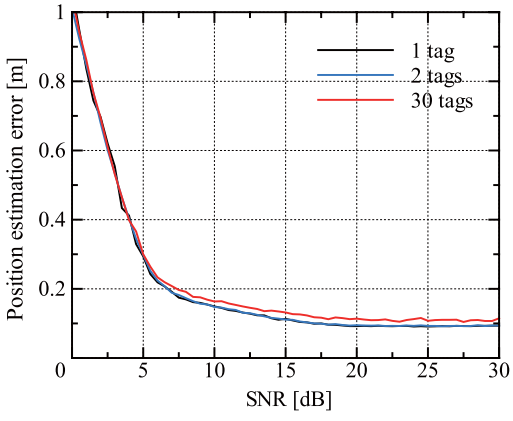

(b) position estimation error

Fig. 12 Comparison of errors in the cases of multiple tags, by the proposed method ($P = 2$).

have functions of tuning TDOA values and transmitting signals to location estimation server via wired or wireless communication. The transmitter tags only have a function of transmitting signals with low power consumption, which can be implemented by omni-directional patch antenna.

Acknowledgments

This work was supported in part by the Murata Science Foundation and the Japan Society for the Promotion of Science (JSPS) Grant-in-Aid for Scientific Research #16K06381. The authors are grateful for their support. Also they thank to anonymous reviewers for valuable comments.

References

[1] D. Bartlett, Essentials of Positioning and Location Technology, Cambridge University Press, 2013.
[2] X. Meng, Z. Ding, and J. Xu, Moving Objects Management: Models, Techniques and Applications, 2nd Ed., Springer, 2014.
[3] A. Dearden, Y. Demiris, and O. Grau, "Tracking football player movement from a single moving camera using particle filters," Proc. European Conf. Visual Media Production, pp.29–37, 2006.
[4] A. Salarpour, "Vehicle tracking using Kalman filter and features," International Journal of Signal and Image Processing, vol.2, no.2, pp.1–8, June 2011.
[5] W.L. Lu, J.A. Ting, J.J. Little, and K.P. Murphy, "Learning to track and identify players from broadcast sports videos," IEEE Trans. Pattern Anal. Mach. Intell., vol.35, no.7, pp.1704–1716, July 2013.
[6] B. Sahbani and W. Adiprawita, "Kalman filter and iterative-Hungarian algorithm implementation for low complexity point tracking as part of fast multiple object tracking system," Proc. Int'l Conf. System Engineering and Technology, Oct. 2016.
[7] T. Von der Grun, N. Franke, D. Wolf, N. Witt, and A Eidloth, "A real-time tracking system for football match and training analysis," in Microelectronic Systems, Circuits, Systems and Applications, pp.199–212, Dec. 2011.
[8] S. Haykin, Adaptive Filter Theory, 4th Ed., Prentice-Hall, 2002.
[9] L. Farhi, "Dynamic location estimation by Kalman filter," Ubiquitous Computing and Communication Journal, vol.7, no.5, pp.1309–1315, March 2010.
[10] C. Chiang, "Hybrid unified Kalman tracking algorithms for heterogeneous wireless location systems," IEEE Trans. Veh. Technol., vol.61, no.2, pp.702–715, Feb. 2011.
[11] Y. Zhao and M. Kyas, "Comparing centralized Kalman filter schemes for indoor positioning in wireless sensor networks," Proc. Int'l Conf. Indoor positioning and Indoor Navigation, pp.1–10, Oct. 2011.
[12] M. Pelka, C. Bollmeyer, and H. Hellbruck, "Accurate radio distance estimation by phase measurements with multiple frequencies," Proc. Int'l Conf. Indoor positioning and Indoor Navigation, pp.142–151, Oct. 2014.
[13] O. Shibata and K. Ichige, "Location estimation system and computer program," patent applied.

Koichi Ichige received B.E., M.E. and Dr. Eng. degrees in Electronics and Computer Engineering from the University of Tsukuba in 1994, 1996 and 1999, respectively. He joined the Department of Electrical and Computer Engineering, Yokohama National University as a research associate in 1999, where he is currently an associate professor. He has been on leave to Swiss Federal Institute of Technology Lausanne (EPFL), Switzerland as a visiting researcher in 2001–2002. His research interests include digital signal processing, approximation theory and their applications to image processing and mobile communication. He served as an associate editor of IEEE Transactions on Industrial Electronics in 2004–2008, Journal of Circuits, Systems and Computers (JCSC) in 2012–2014, and IEICE Transactions on Fundamentals of Electronics, Communications and Computer Sciences in 2015–2018. He received "Meritorious Award on Radio" from the Association of Radio Industries and Businesses (ARIB) in 2006, and Best Letter Award from IEICE Communication Society in 2007. He is a member of IEEE.

Nobuya Arakawa received B.E. and M.E. degrees in Electrical and Computer Engineering from Yokohama National University in 2015 and 2017, respectively. He joined Murata Manufacturing Co., Ltd. and is currently working on research of millimeter wave wireless communications. His research interests include moving object tracking and location estimation techniques.

Ryo Saito received the B.E. degree in Electrical and Computer Engineering from Yokohama National University in 2017. Currently he is a graduate student at the same university. His research interests include FMCW-MIMO radar and location estimation techniques.

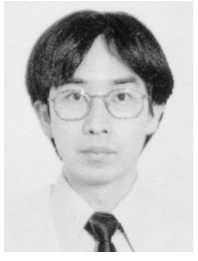

Osamu Shibata received B.E., M.E. and Ph.D. degrees in engineering from Saitama University in 1991, 1993 and 2003 respectively. From 1993 to 2003 he joined Toshiba Corporation and during 1995 to 1998, he was transferred to ATR Optical and Radio Communications Research Laboratories and ATR Adaptive Communications Research Laboratories on leave from Toshiba Corporation. In 2003, he joined Murata Manufacturing Co., Ltd. and is currently working on research of microwave and millimeter wave wireless communications. He received the TELECOM System Technology Award for Student form The Telecommunications Advancement Foundation of Japan in 1994, the Young Engineering Award from IEICE in 1996, and the Best Paper Award from IEICE in 2002 respectively.